

ARTICLE OPEN



Sox13 and M2-like leukemia-associated macrophages contribute to endogenous IL-34 caused accelerated progression of acute myeloid leukemia

Dongyue Zhang^{1,2}, Xiaoxi Cui^{1,2}, Yifei Li^{1,2}, Rong Wang^{1,2}, Hao Wang^{1,2}, Yibo Dai^{1,2}, Qian Ren^{1,2}, Lina Wang^{1,2} and Guoguang Zheng^{1,2}✉

© The Author(s) 2023

Interleukin 34 (IL-34) mainly plays physiologic and pathologic roles through the sophisticated multi-ligand signaling system, macrophage colony-stimulating factor (M-CSF, CSF-1)/IL-34-CSF-1R axis, which exhibits functional redundancy, tissue-restriction and diversity. This axis is vital for the survival, differentiation and function of monocytic lineage cells and plays pathologic roles in a broad range of diseases. However, the role of IL-34 in leukemia has not been established. Here MLL-AF9 induced mouse acute myeloid leukemia (AML) model overexpressing IL-34 (MA9-IL-34) was used to explore its role in AML. MA9-IL-34 mice exhibited accelerated disease progression and short survival time with significant subcutaneous infiltration of AML cells. MA9-IL-34 cells showed increased proliferation. In vitro colony forming assays and limiting dilution transplantation experiments demonstrated that MA9-IL-34 cells had elevated leukemia stem cell (LSC) levels. Gene expression microarray analysis revealed a panel of differential expressed genes including Sex-determining region Y (SRY)-box 13 (Sox13). Furthermore, a positive correlation between the expressions of IL-34 and Sox13 was detected human datasets. Knockdown of Sox13 rescued the enhanced proliferation, high LSC level and subcutaneous infiltration in MA9-IL-34 cells. Moreover, more leukemia-associated macrophages (LAMs) were detected in MA9-IL-34 microenvironment. Additionally, those LAMs showed M2-like phenotype since they expressed high level of M2-associated genes and had attenuated phagocytic potential, suggesting that LAMs should also contribute to IL-34 caused adverse phenotypes. Therefore, our findings uncover the intrinsic and microenvironmental mechanisms of IL-34 in AML and broadens the knowledge of M-CSF/IL-34-CSF-1R axis in malignancies.

Cell Death and Disease (2023)14:308; <https://doi.org/10.1038/s41419-023-05822-z>

INTRODUCTION

Acute myeloid leukemia (AML) is the most common type of acute leukemia in adults [1]. Although clinical treatment has been greatly improved, most AML patients eventually experience relapse and death. As a highly heterogeneous disease, both intrinsic and microenvironmental abnormalities participate in the transformation, progression and relapse of AML [2–4]. Elucidating the mechanisms causing adverse phenotypes of AML including exuberant proliferation [5], more leukemia stem cells (LSCs) [6, 7], massive extramedullary dissemination [2], etc. will provide clues for better outcome.

Interleukin-34 (IL-34) was first identified as another ligand for colony stimulating factor-1 (CSF-1, also known as macrophage colony-stimulating factor, M-CSF) receptor (CSF-1R, CD115) [8]. Although protein-tyrosine phosphatase (PTP)- ζ and Syndecan-1 are also identified as IL-34 receptors [9], much attention has been paid to CSF-1R [10]. Binding of IL-34 to CSF-1R promotes the proliferation and differentiation of monocytes and macrophages [8, 11], whereas IL-34 deficiency results in the decrease of

Langerhans cells and microglia but not monocytes or macrophages [12] owing to the redundancy in the M-CSF/IL-34-CSF-1R axis. This axis also plays pathologic roles in a broad range of diseases [13]. Abnormal expression of M-CSF isoforms, resulted from alternative splicing and posttranslational modifications [14], and IL-34 was reported in various types of malignancies [15–17]. Both intrinsic and microenvironmental mechanisms have been proposed for this axis in malignancies. Specifically, high level IL-34 not only promotes the proliferation, invasion and chemoresistance of cancer cells [16, 17], but also reprograms tumor associated macrophages (TAMs) to acquire a specific phenotype affecting tumor progression [18]. However, IL-34 lacks sequence similarity with M-CSF [11]. M-CSF and IL-34 have differences at steady state and in diseases [13, 19]. Even different isoforms of M-CSF may have diverse pathologic roles in leukemia [20, 21]. These facts reveal the complexity of this axis. Until now, the role of IL-34 in leukemia, especially on LSCs, remains unknown.

Sex-determining region Y (SRY)-box 13 (Sox13), a member of the SRY-related high mobility group (HMG) box (SOX) proteins,

¹State Key Laboratory of Experimental Hematology, National Clinical Research Center for Blood Diseases, Haihe Laboratory of Cell Ecosystem, Institute of Hematology & Blood Diseases Hospital, Chinese Academy of Medical Sciences & Peking Union Medical College, 288 Nanjing Road, Tianjin 300020, China. ²Tianjin Institutes of Health Science, Tianjin 301600, China. ✉email: zhenggtjchn@aliyun.com
Edited by Professor Marc Diederich

Received: 16 November 2022 Revised: 13 April 2023 Accepted: 19 April 2023

Published online: 06 May 2023

plays essential roles in embryonic development, cell fate decision and cancer development [22]. Sox13 promotes the proliferation, migration and metastasis of cancer cells through different mechanisms [23–26]. Recent evidence demonstrated that Sox13 maintained stem-like properties in hepatocellular carcinoma [27]. However, little is known about its pathologic roles in blood diseases. Furthermore, the link between IL-34 and Sox13 have not been established.

In this study, MLL-AF9 induced mouse AML model overexpressing IL-34 was used to explore the role of IL-34 in AML. Overexpression of IL-34 in AML cells accelerates AML progression by promoting cell proliferation and elevating LSC frequency. Furthermore, Sox13 contributes to the pro-leukemic effects in AML cells overexpressing IL-34. Moreover, increased infiltration of M2-like leukemia-associated macrophages (LAMs) with attenuated phagocytic potential may also contribute to the accelerated progression.

MATERIALS AND METHODS

Mouse AML models

The establishment of mouse AML model overexpressing IL-34 is shown in Fig. 1A. Briefly, GFP⁺ AML cells were sorted from MLL-AF9 induced AML mice [28, 29] and infected with blank (pMSCV-PGK-BFP) or IL-34 (pMSCV-IL-34-PGK-BFP) retrovirus. The GFP⁺BFP⁺ leukemia cells, named MA9 and MA9-IL-34 cells, were sorted and transplanted into C57BL/6 J mice by tail intravenous injection to establish MA9 and MA9-IL-34 mice.

To knockdown (KD) Sox13 in MA9-IL-34 cells, validated small hairpin (shRNA) lentivirus targeting mouse Sox13 (the sequences is 5'CCG GGGATGTCAAAGGGACC CAAGACTCGAGTCTGGGTCCCTTGACATCCTTT TGTG3') was constructed using pLKO.1-puro-mcherry vector by IBSBIO technology Inc. MA9-IL-34 cells were infected with scramble (pLKO.1-S-sc) or KD (pLKO.1-S-sh1) lentivirus. The GFP⁺BFP⁺RFP⁺ cells, named IL-34-S-sc and IL-34-S-sh1 cells, were sorted and transplanted into C57BL/6 J mice to establish IL-34-S-sc and IL-34-S-sh1 mice.

Cell cycle and apoptosis assays

In Ki-67 assays, 1×10^6 AML cells were sorted, fixed and permeabilized by Cytofix/Cytoperm™ Fixation/Permeabilization Solution Kit (BD, San Jose, CA). Then, the cells were stained with PE-conjugated Ki-67 for 30 min. Hoechst 33342 was added before flow cytometry analysis.

In BrdU incorporation assays, AML mice were intraperitoneally injected with 200 μ l BrdU (10 mg/ml). 3×10^6 AML cells were sorted 16 h later and stained with a Pharmingen™ APC BrdU Flow Kit (BD, San Jose, CA) following the manufacturer's protocols before flow cytometry analysis.

In apoptosis assays, single cell suspension was prepared with Annexin V binding buffer and incubated with APC-conjugated Annexin V antibody for 15 min in the dark. Then, PI (500 μ g/ml) was added and cells were detected by flow cytometry.

Colony forming assay

Cells were sorted and resuspended in M3434 complete medium. Five hundred cells in 500 μ l were plated into 24-well plate. After seven days, colonies were scanned and counted by a high-content analysis system (PerkinElmer, UK). The colonies were divided into three types according to their morphology: the type A colonies have a dense center and smooth edge; the type B colonies have a compact center and unsmooth edge with migrating cells; the type C colonies have relatively loose structure.

Limiting-dilution transplantation

After sorting, 5×10^2 to 5×10^4 MA9 or MA9-IL-34 cells were transplanted into C57BL/6 J mice. The survival of the mice was recorded. The frequency of LSCs was calculated using extreme limiting dilution analysis (ELDA) online software.

Gene expression microarray

The MA9-c-Kit⁻, MA9-c-Kit⁺ and MA9-IL-34 AML cells were sorted by flow cytometry. Microarrays were completed following standard protocols in Shanghai Majorbio Biopharm Technology (China). Standard analyses were performed by the online Majorbio Cloud Platform. Fold change (FC) ≥ 2.0 and *p* adjust < 0.05 were used as the cutoff for screening differentially expressed genes (DEGs).

Statistical analysis

All experiments were repeated two to three times. The results were represented as means \pm S.E.M. GraphPad Prism 8.0 (GraphPad Software, CA) were used for data analysis. When parameters followed Gaussian distribution, unpaired Student's *t* test was used for comparisons between two groups, whereas one-way ANOVA was used for comparisons among multiple groups. Kaplan–Meier estimates were used for survival curves. ELDA was used for the limiting-dilution transplantation experiments. *P* < 0.05 was considered statistically significant.

RESULTS

MA9-IL-34 cells cause accelerated AML progression

To study the role of IL-34 in AML progression, the MLL-AF9 induced AML model overexpressing IL-34 was established (Fig. 1A). The expression of IL-34 was verified by qRT-PCR, Western blot and ELISA (Figs. S1A–C, S2A–B). Both MA9 and MA9-IL-34 cells were GFP⁺BFP⁺CD3⁺CD19⁺CD11b⁺Gr-1⁺ (Fig. S1D). The expression of IL-34 receptors was also studied. CD115 was detectable at mRNA and protein levels, Syndecan-1 was detectable at mRNA level whereas PTP- ζ was undetectable (Fig. S1E, F). Wright staining showed that MA9-IL-34 cells had larger nucleoli, less but darker cytoplasm than MA9 cells (Figure S1G). MA9-IL-34 mice exhibited higher levels of PB leukemia cells since day 13 (Fig. 1B) and shorter survival times than MA9 mice (Fig. 1C). Hepatosplenomegaly was more severe in MA9-IL-34 mice than MA9 mice on day 17 (Fig. 1D, E). Furthermore, pathologic analysis showed that more infiltrating AML cells were observed in tissues from MA9-IL-34 mice than MA9 mice. Interestingly, subcutaneous infiltration of AML cells was observed in MA9-IL-34 mice (Fig. 1F, Fig. S1H). These results suggested that overexpression of IL-34 in AML cells accelerated AML progression.

Characteristics of MA9-IL-34 cells

To explore the mechanism leading to the accelerated AML progression, the characteristics of AML cells were first studied. BrdU assay showed that more S and G2/M phase but fewer G0/G1 phase cells were detected in MA9-IL-34 cells than MA9 cells (Fig. 2A). The apoptotic rate between two groups had no significant difference (Fig. 2B). Colony forming potential partly reflects the LSC level, which is associated with poor prognosis in AML. The in vitro colony forming experiments demonstrated that MA9-IL-34 cells formed more colonies than MA9 cells in both primary and secondary plating experiments (Fig. 2C, D). There are three types of colonies (Figure S3) [3, 30]. MA9-IL-34 cells formed more type A and type B colonies than MA9 cells in primary plating experiment. Similar results were also obtained in secondary plating experiments (Fig. 2C, D). Limiting dilution transplantation experiments were used to analyze LSC frequency. 5×10^4 or 5×10^3 cells caused 100% death in both groups. 5×10^2 cells caused 80% death in MA9-IL-34 group but 40% in MA9 group (Fig. 2E). The LSC level in MA9-IL-34 cells was approximately 2-fold higher than that in MA9 cells (Fig. 2F). The expression of c-Kit, an important marker of LSCs, was detected by flow cytometry. More than 90% MA9-IL-34 cells whereas approximately half MA9 cells were c-Kit⁺ (Fig. 2G). Equal numbers of MA9-c-Kit⁻, MA9-c-Kit⁺ and MA9-IL-34 cells were sorted and transplanted into recipient mice. As expected, MA9-IL-34 mice had the shortest survival time (Fig. 2H). Taken together, AML cells overexpressing IL-34 have enhanced proliferation and elevated LSC frequency, which contribute to the accelerated AML progression.

Identification of intrinsic molecules contributing to the pro-leukemic effects in MA9-IL-34 cells

MA9-c-Kit⁻, MA9-c-Kit⁺ and MA9-IL-34 cells were undergone expression microarray to screen intrinsic key molecules contributing to the accelerated disease progression. A Venn diagram shows the numbers of DEGs between different pairs of the samples (Fig. 3A). The number of DEGs between MA9-IL-34 and MA9-c-Kit⁻ was greater than that between MA9-IL-34 and MA9-c-Kit⁺, which

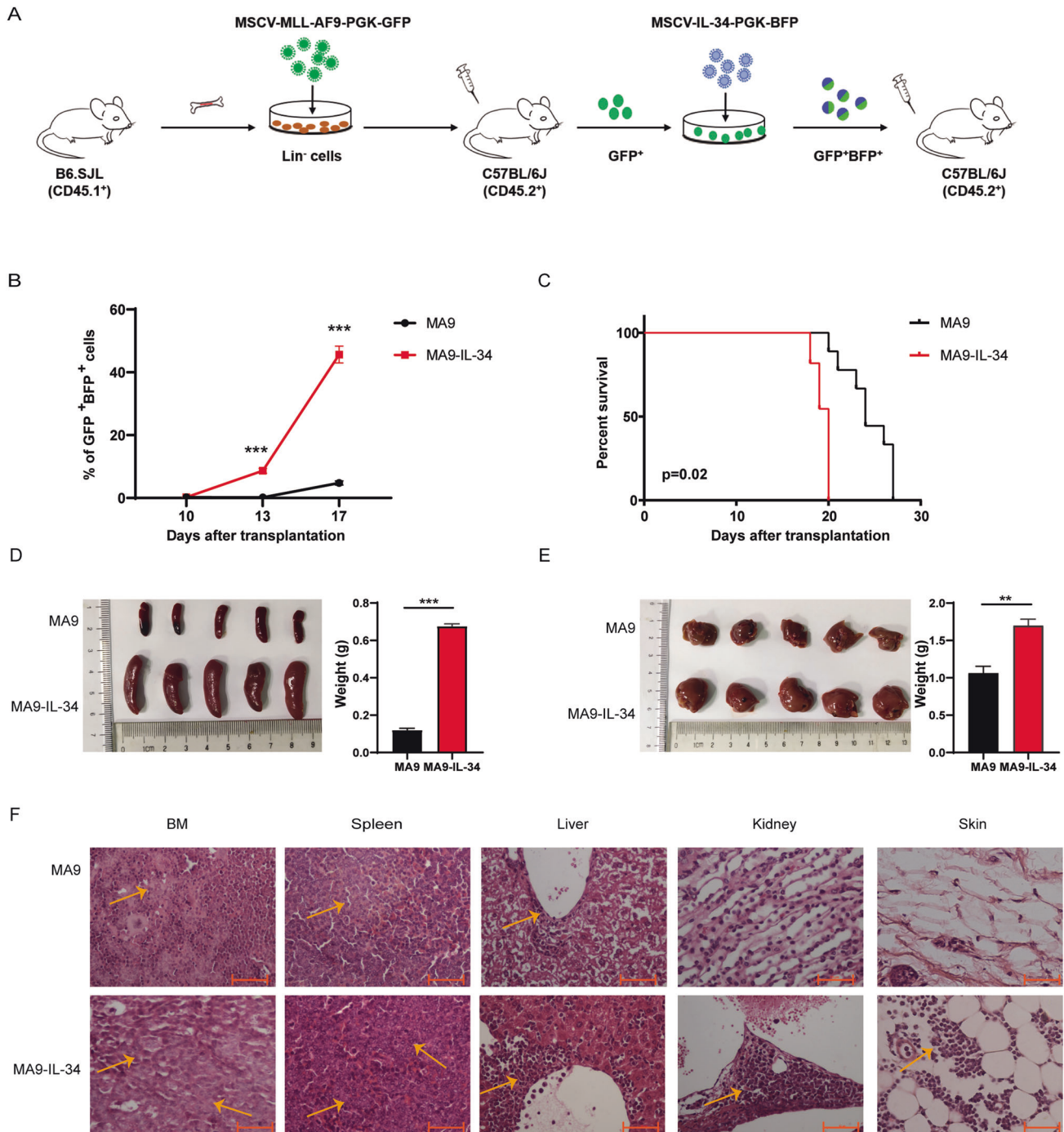


Fig. 1 Overexpression of IL-34 accelerated AML progression. **A** Schematic overview showing the establishment of the MA9 and MA9-IL-34 mouse AML models. **B–F** 1×10^5 GFP⁺BFP⁺ cells were transplanted into recipient mice and the progression of AML was studied. **B** The PB leukemia cell levels were monitored at indicated time points ($n = 4$). **C** The survival of AML mice is shown in Kaplan-Meier curves (MA9, $n = 10$; MA9-IL-34, $n = 11$). **D–E** The size and weight of spleens (**D**) and livers (**E**) on day 17 are shown. **F** The HE-stained sections of BM, spleen, liver, kidney and skin were examined under a light microscope. Scale bars: 50 μ m. Data are presented as mean \pm S.E.M. Unpaired Student's *t* test and Kaplan-Meier estimates were used. ** $p < 0.01$, *** $p < 0.001$.

was in accordance with functional observations. GSEA analysis showed that the genes in annotations "quiescent up", "cell cycle checkpoints" and "G2/M checkpoints" were enriched in MA9-IL-34 cells versus MA9-c-Kit⁺ or MA9-c-Kit⁻ cells (Fig. 3B). Furthermore, genes in annotations related to worse phenotypes in tumors were enriched in MA9-IL-34 cells versus MA9-c-Kit⁺/MA9-c-Kit⁻ (Fig. S4A) or MA9-c-Kit⁺ cells (Fig. S4B). Moreover, embryonic stem cell core associated genes were enriched in MA9-IL-34 cells versus MA9-c-

Kit⁻ cells (Fig. S4C). The 1572 genes (DEGs between MA9-IL-34 and MA9-c-Kit⁺ cells) were divided into 4 clusters based on their expression pattern in three groups. The cluster I with 428 genes was of interest (Fig. 3C). Then, 126 genes were first selected since they were also DEGs between MA9-c-Kit⁺ and MA9-c-Kit⁻ groups, furthermore the expression was higher in MA9-c-Kit⁺ cells than MA9-c-Kit⁻ cells. Five genes with high expression levels, which related to stemness of tumor cells, were selected and further

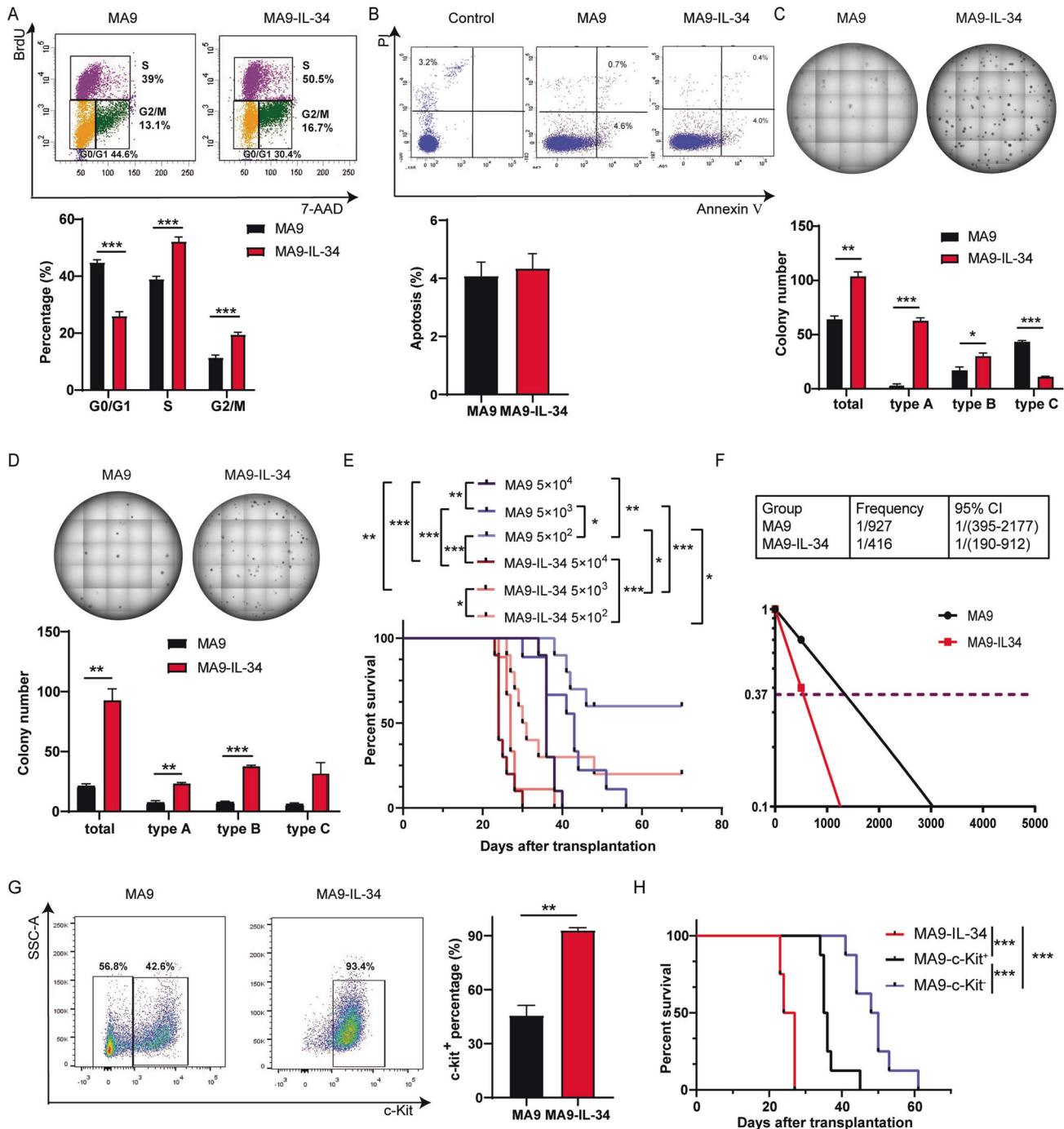


Fig. 2 The characteristics of MA9-IL-34 cells. **A–D** The mice were transplanted with MA9 or MA9-IL-34 cells on day 0 and sacrificed on day 16. **A** Mice were sacrificed 16 h after intraperitoneal injection of 200 μ g BrdU. Then assays were performed following standard protocols. The representative flow cytometric results are shown (upper), and the percentages of G0/G1-, S- and G2/M-phase AML cells are plotted (lower). **B** Annexin V and PI staining was performed following standard protocols. The representative flow cytometric results are shown (upper), and the percentage of apoptotic AML cells is plotted (lower). **C–D** Primary (**C**) and secondary (**D**) colony forming assays were performed when 500 AML cells in M3434 medium were seeded each well into 24-well plates and cultured for 7d. The representative results are shown (upper), and colony numbers are plotted (lower). **E, F** Different numbers of sorted AML cells (5×10^4 , 5×10^3 , 5×10^2 for each group) were transplanted into recipient mice ($n = 9$ to 10 for each group). The survival of mice is shown in Kaplan–Meier curves (**E**). The frequency of LSCs was calculated using ELDA software (**F**). **G** AML cells were stained with c-Kit. The representative flow cytometric results are shown (left), and the percentage of c-Kit⁺ cells is plotted (right). **H** Equal numbers of sorted MA9-c-Kit⁺, MA9-c-Kit⁺ and MA9-IL-34 cells were transplanted into recipient mice. The survival of mice is shown in Kaplan–Meier curves ($n = 8$ for each group). Data are presented as mean \pm S.E.M. Unpaired Student's *t* test, one-way ANOVA tests and Kaplan–Meier estimates were used. * $p < 0.05$, ** $p < 0.01$, *** $p < 0.001$.

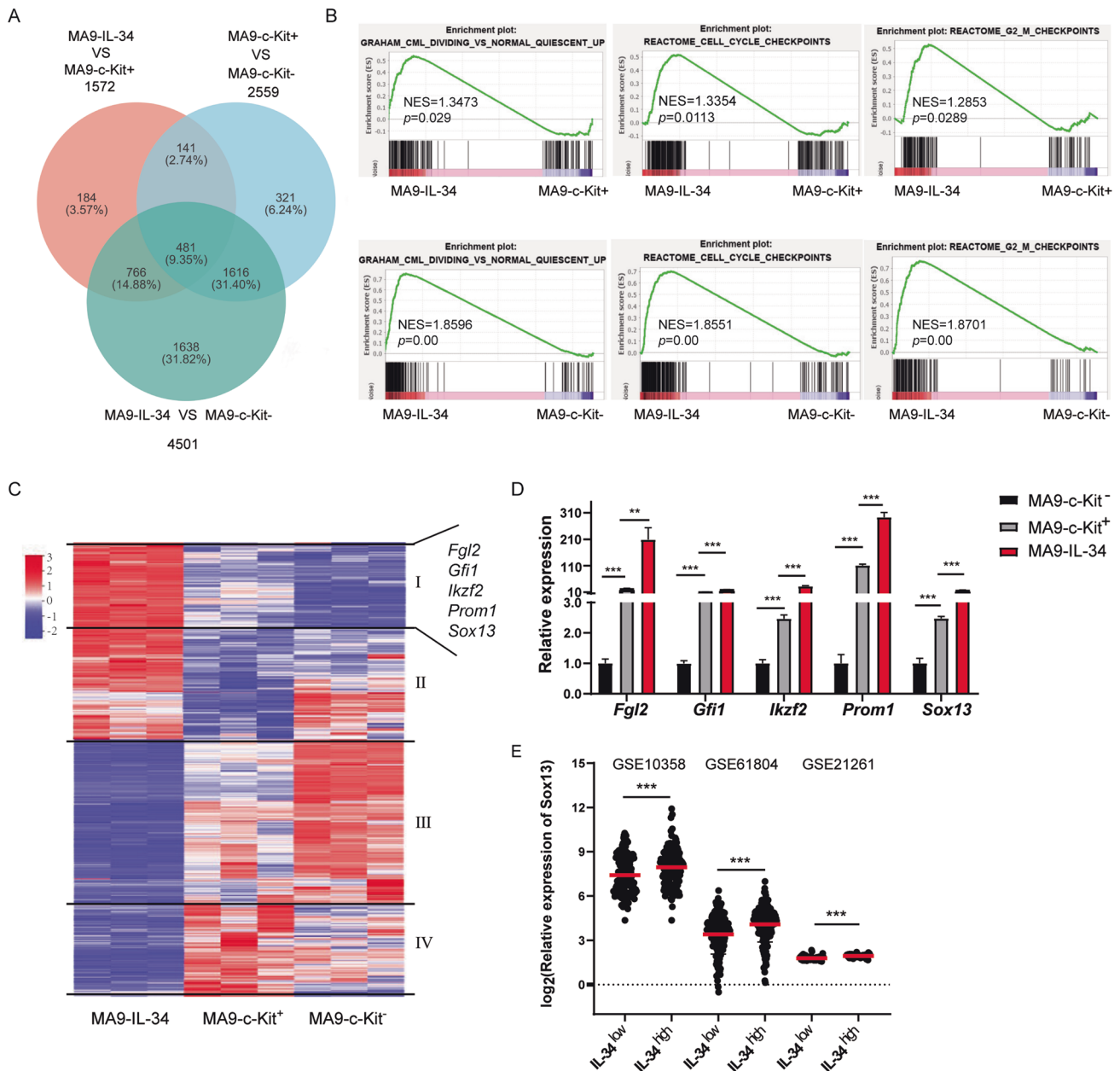


Fig. 3 Identification of intrinsic molecules contributing to the pro-leukemic effects in MA9-IL-34 cells. MA9-c-Kit⁻, MA9-c-Kit⁺, MA9-IL-34 cells were sorted and microarray was performed. **A** Venn diagram shows overlaps of DEGs obtained from each pair. **B** GSEA analysis shows the enrichment of genes in annotations between MA9-IL-34 and MA9-c-Kit⁺/MA9-c-Kit⁻ groups. **C** Heat map shows the expression levels of 1572 genes, which are the DEGs between MA9-IL-34 and MA9-c-Kit⁺ groups, in three groups. Those genes are subdivided into 4 clusters based on the expression patterns in three groups. **D** The expression of selected genes was validated by qRT-PCR. **E** The expression level of Sox13 in the GSE10358 ($n = 304$), GSE61804 ($n = 324$) and GSE21261 ($n = 76$) is shown. For each dataset, AML cases were divided into IL-34^{low} and IL-34^{high} groups, and the corresponding expression of Sox13 is plotted. Data are presented as mean \pm S.E.M. Unpaired Student's *t* test, one-way ANOVA tests were used. ** $p < 0.01$, *** $p < 0.001$.

verified by qRT-PCR (Fig. 3D). Notably, a significant positive correlation between the expression of *IL-34* and *SOX13* was detected in the human datasets GSE10358, GSE21261 and GSE61804 (Fig. 3E). Hence, *Sox13* was selected for further study.

Sox13 contributes to the pro-leukemic effects in MA9-IL-34 cells

To investigate whether *Sox13* contributed to the malignant phenotype, MA9-IL-34 cells were infected with pLKO.1-S-sc or pLKO.1-S-sh1 to construct IL-34-S-sc and IL-34-S-sh1 mouse AML models. The knockdown efficiency of *Sox13* was verified by qRT-PCR (Fig. 4A). IL-34-S-sc and IL-34-S-sh1 cells were both

GFP⁺BFP⁺RFP⁺CD3⁺CD19⁺Gr-1⁺CD11b⁺ (Fig. S5A, B). The IL-34-S-sh1 mice exhibited lower PB leukemia cell levels since day 16 after transplantation (Fig. 4B) and had longer survival times than IL-34-S-sc mice (Fig. 4C). Hepatosplenomegaly was milder (Fig. 4D) and fewer infiltrating AML cells (Fig. S5C) were detected in liver in IL-34-S-sh1 mice than IL-34-S-sc mice on day 19. Pathologic analysis showed that subcutaneous infiltration of AML cells was observed in IL-34-S-sc mice but not IL-34-S-sh1 mice although leukostasis was observed in subcutaneous blood vessels in IL-34-S-sh1 mice (Fig. S5D). Ki-67 experiments showed that more G1 phase cells and fewer S/G2/M phase cells were detected in IL-34-S-sh1 cells (Fig. 4E). Knockdown of *Sox13* resulted in the decreased expression of c-Kit

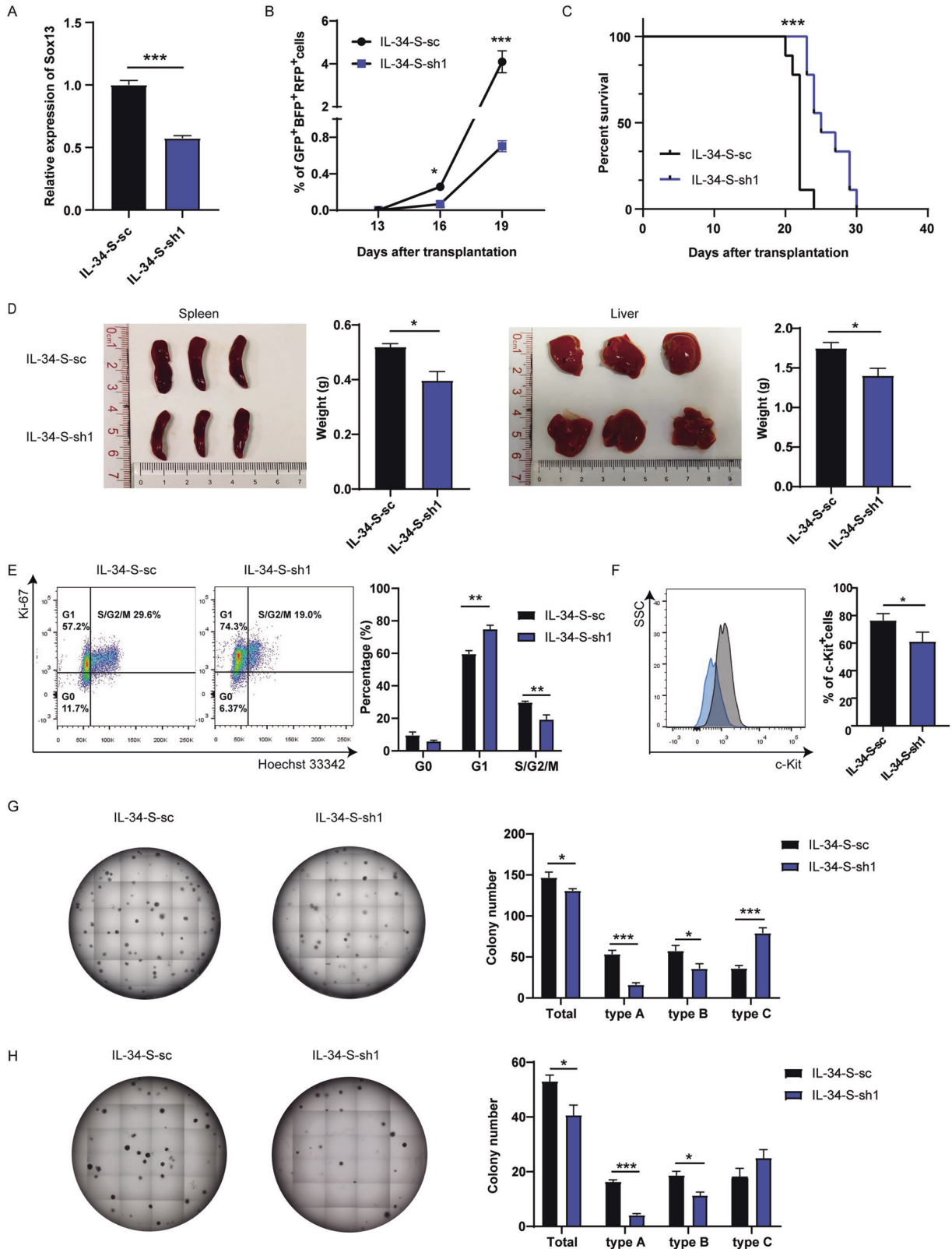


(Fig. 4F). Furthermore, *in vitro* colony forming assay showed that IL-34-S-sh1 cells formed fewer colonies than IL-34-S-sc cells in primary and secondary plating experiments (Fig. 4G, H). Taken together, these results suggest that Sox13 acts as intrinsic factor contributing to the pro-leukemic effects in AML mice overexpressing IL-34.

LAMs contribute to the pro-leukemic effects in MA9-IL-34 mice

Immunologic microenvironment plays important roles in leukemia progression [31, 32]. No significant difference was detected on the distribution of B cells, NK cells, CD4⁺ cells and CD8⁺ T cells in spleen

Fig. 4 Sox13 contributes to the pro-leukemic effects in MA9-IL-34 cells. The expression of Sox13 was knocked down in MA9-IL-34 cells by shRNA strategy. **A** The expression of Sox13 was detected by qRT-PCR. **B–D** Equal numbers of IL-34-S-sc or IL-34-S-sh1 cells were sorted and transplanted into recipient mice. **B** The PB AML cells were monitored at indicated time points ($n = 4$). **C** The survival of mice is shown in Kaplan–Meier curves ($n = 9$ for each group). **D** The sizes and weights of spleens and livers on day 19 are shown. **E** IL-34-S-sc or IL-34-S-sh1 cells were stained with Ki-67 and Hoechst 33342. The representative flow cytometric results are shown (left), and the percentages of G0-, G1-, and S/G2/M-phase AML cells are plotted (right). **F** GFP⁺BFP⁺RFP⁺ cells were stained with c-Kit. The representative flow cytometric results are shown (left), and the percentages of c-Kit⁺ cells are plotted. **G, H** Primary (**G**) and secondary (**H**) colony forming assays were performed when 500 AML cells in M3434 medium were seeded each well into 24-well plates and cultured for 7d. The representative results are shown (left), and the colony numbers are plotted (right). Data are presented as mean \pm S.E.M. Unpaired Student's *t* test, one-way ANOVA tests and Kaplan–Meier estimates were used. * $p < 0.05$, ** $p < 0.01$, *** $p < 0.001$.

samples as well as granulocytes in BM samples (Fig. S6 A–D). Signaling through CSF-1R, the major receptor of IL-34, is vital for the differentiation and survival of mononuclear phagocytes; and macrophages play important roles in malignancies including leukemia [33–36]. The macrophages in BM and spleen were gated as the SSC^{int/lo} subpopulation in the CD3^{Gr-1^{lo}F4/80⁺CD115^{int}} population while those in liver were gated as the CD11b⁺F4/80⁺CD45⁺ population [36] (Fig. 5A, B). Higher levels of LAMs were detected in those tissues in MA9-IL-34 mice than MA9 mice (Fig. 5C). Furthermore, it is well accepted that M1 macrophages have anti-tumor effects whereas M2 macrophages have pro-tumor effects [34]. LAMs from MA9-IL-34 mice expressed higher levels of M2-associated genes including *Cd206*, *Arg1*, *Il-10* and *Mmp9* than MA9 mice, whereas expressed similar levels of M1-associated genes as MA9 mice (Fig. 5D). We used a multiple factor weight comprehensive analysis to define the activation phenotype of LAMs [33, 36]. The results showed that LAMs in MA9-IL-34 microenvironment have more M2 characteristics (Fig. S6E), or simply called as M2-like LAMs. Moreover, phagocytosis is an important anti-tumor function of macrophages [21, 37, 38]. LAMs in MA9-IL-34 mice had lower phagocytic potential than those in MA9 mice (Fig. 5E). Taken together, there are more M2-like LAMs with lower phagocytic potential in MA9-IL-34 microenvironment, which suggest that LAM-associated microenvironmental mechanisms should also contribute to the pro-leukemic effects in MA9-IL-34 mice.

Pexidartinib partly attenuates AML progression in MA9-IL-34 mice

Pexidartinib, the CSF-1R inhibitor, was used to test the effects in MA9-IL-34 mice (Fig. S7A). Pexidartinib decreased the weight of spleen and liver, in MA9-IL-34 mice (Fig. S7B). Additionally, it suppressed subcutaneous infiltration of AML cells in MA9-IL-34 mice (Fig. S7C). Moreover, it significantly lowered the AML cell burden in BM and SP (Fig. S7D). Furthermore, it downregulated the expression of c-kit in MA9-IL-34 cells (Fig. S7E). Besides, it lowered the level of LAMs in BM and spleen in MA9-IL-34 mice (Fig. S7F). Prolong in survival time was not observed (Fig. S7G), which may be partly due to rapid progression of MLL-AF9-induced AML model and incomplete blockage of excessive IL-34 by the recommended dosage of Pexidartinib. Therefore, M-CSFR inhibitor partly attenuated the progression of MA9-IL-34 mice.

DISCUSSION

The development of malignancies is regulated by complex networks comprising both intrinsic and microenvironmental factors. The effect of M-CSF/IL-34-CSF-1R axis in malignancies is a good example since it covers both aspects. In fact, abnormal expression and function of both ligands and receptor were reported in various malignancies including pre-leukemia, leukemia and lymphoid malignancies [10, 17, 39]. Furthermore, abnormal activation of this axis may directly stimulate malignant cells and/or shape immunologic microenvironment [15, 40, 41]. Notably, this axis is vital for monocytic lineage cells, either normal or malignant. Therefore, acute myelomonocytic leukemia, such as the MLL-rearranged AML [42], is a good model to elucidate the mechanism of this axis in malignancies.

However, the multiple-ligand axis exhibits expressional and functional diversities under both physiological and pathological conditions. IL-34 is regarded as a tissue-restricted ligand of CSF-1R in skin and central nerve system [12]. Furthermore, M-CSF isoforms, i.e. secretory (sM-CSF), membrane-bound (mM-CSF), and extracellular matrix or proteoglycan (PG-M-CSF), exhibit different expression patterns and functions [43]. While sM-CSF elicits short-term signal and exerts short- or long-distance effects by autocrine, paracrine or endocrine mechanisms, mM-CSF provides persistent activation signal and regulates physically contacted cells by juxtacrine mechanism [43, 44]. We previously demonstrated that macrophages shaped by sM-CSF and mM-CSF showed significant phenotypic diversity; and mM-CSF but not sM-CSF prolonged the survival of AML mice by inducing the differentiation of AML cells and polarizing LAMs to have high phagocytotic potential [20, 21]. Here we report that overexpression of IL-34 in AML cells results in accelerated AML progression, short survival and significant subcutaneous infiltration. Furthermore, Sox13-associated upregulated proliferation and LSC level account for intrinsic mechanism while M2-like LAMs account for microenvironmental mechanism. Hence, our study gives new insight into the pathologic role of IL-34 in AML and broadens the knowledge of the M-CSF/IL-34-CSF-1R axis in malignancies.

The survival and function of cells are tightly regulated by a complex network and a single gene abnormality in malignant cells may frequently lead to several adverse phenotypes [3, 30, 45]. Overexpression of IL-34 in AML cells simultaneously causes enhanced malignant proliferation, more LSCs and significant subcutaneous infiltration. MLL-AF9 induced AML is a good model for monocytic lineage malignancies [28] and the M-CSF/IL-34-CSF-1R axis provides signals to boost malignant proliferation. Overexpression of IL-34 in human MLL-rearranged cell lines, THP1 and Momi1-3, also have pro-proliferative effect [46]. In fact, IL-34 is abnormally expressed and promotes malignant proliferation in different types of cancers [16, 17, 47, 48]. Therefore, although the physiologic significance of IL-34 seems to be tissue-restricted, abnormally expressed IL-34 can provide pro-proliferative signals in a broad range of malignancies.

LSCs are responsible for the initiation, drug resistance, relapse and bad outcome in leukemia [7, 49]. A novel finding of this study is that overexpression of IL-34 in AML cells increases LSC frequency. Nowadays, there is not a good method to mark LSCs although the mouse L-GMP, the typical markers of which is IL-7R⁺Lin⁺Sca-1⁻c-Kit⁺CD34⁺FcgRII/III⁺, is suggested [50]. However, L-GMP frequency is not suitable for this particular model [3, 30] since considerable S-phase L-GMPs were detected either in reports [45] or from our observations, demonstrating that at least part of L-GMPs are proliferative instead of quiescent. Furthermore, most AML cells in this model were Gr-1⁺ but not the Lin⁺ cells so that L-GMP in MA9-IL-34 cells can hardly be gated and the G0/G1 phase L-GMP level is lower than LSC level obtained from functional experiments. Most importantly, the conclusion is obtained based on the functional experiments, i.e. the colony forming and limiting dilution transplantation experiments. There may be another question, i.e. enhanced proliferation and high LSC level seem to be controversial because LSCs/tumor stem cells (TSCs) are normally considered as quiescent cells [51, 52]. In fact, malignant cells are composed of

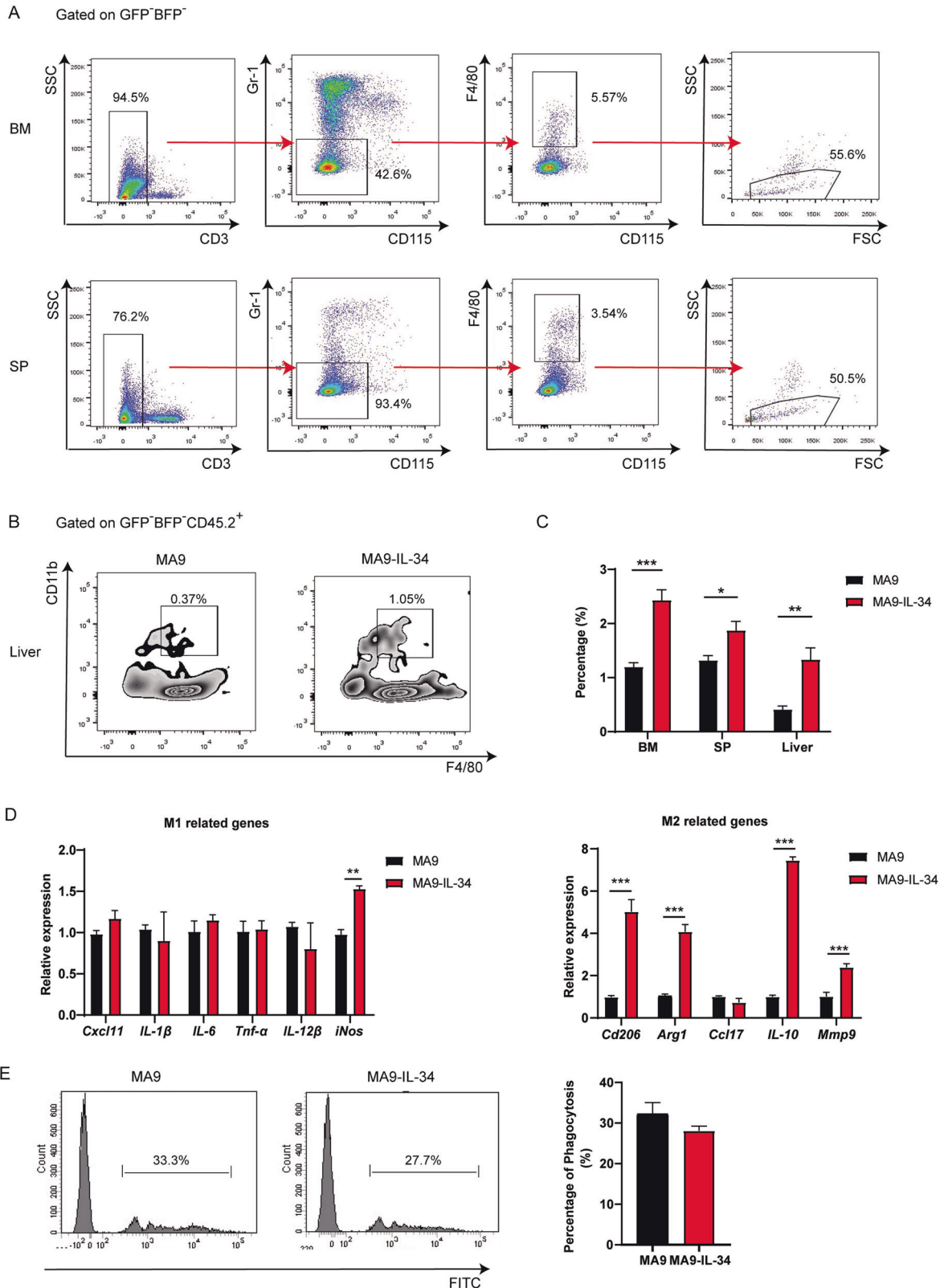


Fig. 5 LAMs contribute to the pro-leukemic effects in MA9-IL-34 mice. AML mice were sacrificed at middle stage of leukemia. BM and SP samples were prepared. **A** Gating strategy for LAMs from BM and SP samples by flow cytometry. **B** Gating strategy for LAMs from liver samples by flow cytometry. **C** The frequencies of LAMs in different tissues are plotted. **D, E** LAMs were sorted from BM samples. The expression of M1- and M2- associated genes in LAMs was detected by qRT-PCR (**D**). The representative flow cytometric results (left) and the positive rates (right) of in vitro uptake experiments to assess the phagocytotic potential of LAMs are shown (**E**). Data are presented as mean \pm S.E.M. Unpaired Student's *t* test, one-way ANOVA tests were used. * $p < 0.05$, ** $p < 0.01$, *** $p < 0.001$.

heterogeneously hierarchical sub-populations [53]. In this case, AML cells can be simply classified into LSCs (small number) and non-LSCs (abundant). Some key molecules may simultaneously participate in the maintenance of LSCs and the proliferation of non-LSCs. In fact, malignancies with both adverse characteristics are frequently observed not only in research models but also in clinical patients [3, 30, 54]. How IL-34 boosts LSCs has not been fully understood although we demonstrate that Sox13 is partly responsible for this.

Subcutaneous infiltration is another pathologic characteristic of MA9-IL-34 cells. It's worth noting that the significant physiologic effects of IL-34 seem to be restricted in skin and central nerve system [12]. However, enhanced intracerebral invasion has not been observed possibly due to the blood brain barrier. Nevertheless, extramedullary infiltration of leukemia cells has long been observed and considered as a bad marker for leukemia patients [2]. Patients suffer combined extramedullary and BM relapse has worse prognosis than those with BM relapse alone [55]. Furthermore, leukemia cutis as a specific extramedullary infiltration signifies a poor prognosis of AML [56, 57]. Therefore, although the mechanism is not clear, this phenomenon accounts for another adverse effect of IL-34 in AML.

The association between IL-34 and Sox13 has not been previously reported. Sox13 at least partly mediates the adverse phenotypes including enhanced proliferation, more LSCs and subcutaneous infiltration in MA9-IL-34 cells. The pro-proliferative effects of Sox13 in solid tumors have been reported and different pathways, such as the Wnt- β -catenin pathway, the SOX13-TRIM11-YAP axis as well as the PAX8-Aurora B/Cyclin B1 pathway, have been proposed [24–26]. Recent observation showed that Sox13 regulated cancer stem-like properties in hepatocellular carcinoma cells but the mechanism was not clear [27]. Therefore, although the pathway from IL-34 to Sox13 and downstream adverse phenotypes has been observed in AML, the molecular mechanisms including how IL-34 regulates the expression of Sox13, the downstream events of Sox13 leading to enhanced proliferation, more LSCs and subcutaneous infiltration have not been elucidated and deserve further exploration.

Macrophages are an important component of the physiologic and pathologic microenvironment and play sophisticated roles in the initiation and progression of malignancies [33, 35, 58]. Although the M1/M2 criteria has obvious limitation, the evidence demonstrating the anti-tumor M1 or M1-like macrophages and the pro-tumor M2 or M2-like macrophages has been well documented [34]. Furthermore, the M-CSF/IL-34-CSF-1R axis is vital for the survival and function of macrophages although different ligand may have diverse effects [19–21, 41]. Here we report that increased LAMs are detected in MA9-IL-34 microenvironment. Whether this phenomenon is caused by increased recruitment and/or local expansion is not clear. Furthermore, those LAMs exhibit more M2 characteristics since they express high level of M2 phenotype associated genes including *Cd206*, *Arg1*, *Il-10* and *Mmp9*, which imply that they may have pro-leukemic effects. Moreover, LAMs in MA9-IL-34 microenvironment exhibit low phagocytic potential, which mediates the anti-tumor effects of macrophages [37, 38]. Thus, more M2-like LAMs are polarized in the MA9-IL-34 microenvironment and at least partly account for the accelerated AML progression.

In conclusion, we demonstrate that IL-34 overexpressed in AML cells accelerates AML progression by affecting both AML cell themselves and LAMs in the leukemia microenvironment. Upregulated Sox13 accounts for the promoted proliferation, increased LSC level and subcutaneous infiltration.

DATA AVAILABILITY

Bulk RNA-seq data are available in the National Center for Biotechnology Information Gene Expression Omnibus database under accession number GSE213201.

REFERENCES

- Arber DA, Orazi A, Hasserjian R, Thiele J, Borowitz MJ, Le Beau MM, et al. The 2016 revision to the World Health Organization classification of myeloid neoplasms and acute leukemia. *Blood*. 2016;127:2391–405.
- Eckardt JN, Stölzel F, Kunadt D, Röhlig C, Stasik S, Wagenführ L, et al. Molecular profiling and clinical implications of patients with acute myeloid leukemia and extramedullary manifestations. *J Hematol Oncol*. 2022;15:60.
- Feng W, Yang X, Wang L, Wang R, Yang F, Wang H, et al. P2X7 promotes the progression of MLL-AF9 induced acute myeloid leukemia by upregulation of Pbx3. *Haematologica*. 2021;106:1278–89.
- Wang R, Feng W, Wang H, Wang L, Yang X, Yang F, et al. Blocking migration of regulatory T cells to leukemic hematopoietic microenvironment delays disease progression in mouse leukemia model. *Cancer Lett*. 2020;469:151–61.
- Culp-Hill R, D'Alessandro A, Pietras EM. Extinguishing the embers: targeting AML metabolism. *Trends Mol Med*. 2021;27:332–44.
- Woll PS, Yoshizato T, Hellström-Lindberg E, Fioretos T, Ebert BL, Jacobsen SEW. Targeting stem cells in myelodysplastic syndromes and acute myeloid leukemia. *J Intern Med*. 2022;292:262–77.
- Wang J, Wang P, Zhang T, Gao Z, Wang J, Feng M, et al. Molecular mechanisms for stemness maintenance of acute myeloid leukemia stem cells. *Blood Sci*. 2019;1:77–83.
- Lin H, Lee E, Hestir K, Leo C, Huang M, Bosch E, et al. Discovery of a cytokine and its receptor by functional screening of the extracellular proteome. *Science*. 2008;320:807–11.
- Baghdadi M, Umeyama Y, Hama N, Kobayashi T, Han N, Wada H, et al. Interleukin-34, a comprehensive review. *J Leukoc Biol*. 2018;104:931–51.
- Monteleone G, Maresca C, Colella M, Pacifico T, Congiu D, Troncone E, et al. Targeting IL-34/M-CSF-1R Axis in Colon Cancer. *Front Immunol*. 2022;13:917955.
- Otsuka R, Wada H, Seino KI. IL-34, the rationale for its expression in physiological and pathological conditions. *Semin Immunol*. 2021;54:101517.
- Wang Y, Szretter KJ, Vermi W, Gilfillan S, Rossini C, Cella M, et al. IL-34 is a tissue-restricted ligand of CSF1R required for the development of Langerhans cells and microglia. *Nat Immunol*. 2012;13:753–60.
- Freuchet A, Salama A, Remy S, Guillonnetau C, Anegon I. IL-34 and CSF-1, deciphering similarities and differences at steady state and in diseases. *J Leukoc Biol*. 2021;110:771–96.
- Nandi S, Akhter MP, Seifert MF, Dai XM, Stanley ER. Developmental and functional significance of the CSF-1 proteoglycan chondroitin sulfate chain. *Blood*. 2006;107:786–95.
- Chockalingam S, Ghosh SS. Macrophage colony-stimulating factor and cancer: a review. *Tumour Biol*. 2014;35:10635–44.
- Irie T, Yoshii D, Komohara Y, Fujiwara Y, Kadohisa M, Honda M, et al. IL-34 in hepatoblastoma cells potentially promote tumor progression via autocrine and paracrine mechanisms. *Cancer Med*. 2022;11:1441–53.
- Franzè E, Marafini I, Troncone E, Salvatori S, Monteleone G. Interleukin-34 promotes tumorigenic signals for colon cancer cells. *Cell Death Disco*. 2021;7:245.
- Kajihara N, Kitagawa F, Kobayashi T, Wada H, Otsuka R, Seino KI. Interleukin-34 contributes to poor prognosis in triple-negative breast cancer. *Breast Cancer*. 2020;27:1198–204.
- Boulakirba S, Pfeifer A, Mhaidly R, Obba S, Goulard M, Schmitt T, et al. IL-34 and CSF-1 display an equivalent macrophage differentiation ability but a different polarization potential. *Sci Rep*. 2018;8:256.
- Liao J, Feng W, Wang R, Ma S, Wang L, Yang X, et al. Diverse in vivo effects of soluble and membrane-bound M-CSF on tumor-associated macrophages in lymphoma xenograft model. *Oncotarget*. 2016;7:1354–66.
- Wang R, Feng W, Yang F, Yang X, Wang L, Chen C, et al. Heterogeneous effects of M-CSF isoforms on the progression of MLL-AF9 leukemia. *Immunol Cell Biol*. 2018;96:190–203.
- Kumar P, Mistri TK. Transcription factors in SOX family: potent regulators for cancer initiation and development in the human body. *Semin Cancer Biol*. 2020;67:105–13.
- Du F, Li X, Feng W, Qiao C, Chen J, Jiang M, et al. SOX13 promotes colorectal cancer metastasis by transactivating SNAIL2 and c-MET. *Oncogene*. 2020;39:3522–40.
- Tang J, Tian Z, Liao X, Wu G. SOX13/TRIM11/YAP axis promotes the proliferation, migration and chemoresistance of anaplastic thyroid cancer. *Int J Biol Sci*. 2021;17:417–29.
- Jin X, Shao X, Pang W, Wang Z, Huang J. Sex-determining Region Y-box transcription factor 13 promotes breast cancer cell proliferation and glycolysis by activating the tripartite motif containing 11-mediated Wnt/ β -catenin signaling pathway. *Bioengineered*. 2022;13:13033–44.
- Bie L, Li D, Wei Y, Li N, Chen X, Luo S. SOX13 dependent PAX8 expression promotes the proliferation of gastric carcinoma cells. *Artif Cells Nanomed Biotechnol*. 2019;47:3180–87.
- Jiao H, Fang F, Fang T, You Y, Feng M, Wang X, et al. SOX13 regulates cancer stem-like properties and tumorigenicity in hepatocellular carcinoma cells. *Am J Cancer Res*. 2021;11:760–72.

28. Somerville TC, Cleary ML. Identification and characterization of leukemia stem cells in murine MLL-AF9 acute myeloid leukemia. *Cancer Cell*. 2006;10:257–68.
29. Cheng H, Hao S, Liu Y, Pang Y, Ma S, Dong F, et al. Leukemic marrow infiltration reveals a novel role for Egr3 as a potent inhibitor of normal hematopoietic stem cell proliferation. *Blood*. 2015;126:1302–13.
30. Wang H, Zhang D, Cui X, Dai Y, Wang C, Feng W, et al. Loss of IRF7 accelerates acute myeloid leukemia progression and induces VCAM1-VLA-4 mediated intracerebral invasion. *Oncogene*. 2022;41:2303–14.
31. Yang F, Wang R, Feng W, Chen C, Yang X, Wang L, et al. Characteristics of NK cells from leukemic microenvironment in MLL-AF9 induced acute myeloid leukemia. *Mol Immunol*. 2018;93:68–78.
32. Moore JA, Mistry JJ, Hellmich C, Horton RH, Wojtowicz EE, Jibril A, et al. LC3-associated phagocytosis in bone marrow macrophages suppresses acute myeloid leukemia progression through STING activation. *J Clin Invest*. 2022;132:e153157.
33. Yang X, Feng W, Wang R, Yang F, Wang L, Chen S, et al. Repolarizing heterogeneous leukemia-associated macrophages with more M1 characteristics eliminates their pro-leukemic effects. *Oncoimmunology*. 2018;7:e1412910.
34. Wang J, Mi S, Ding M, Li X, Yuan S. Metabolism and polarization regulation of macrophages in the tumor microenvironment. *Cancer Lett*. 2022;543:215766.
35. Chen S, Yang X, Feng W, Liao J, Wang L, Feng L, et al. Organ-specific microenvironment modifies diverse functional and phenotypic characteristics of leukemia-associated macrophages in mouse T cell acute lymphoblastic leukemia. *J Immunol*. 2015;194:2919–29.
36. Yang F, Feng W, Wang H, Wang L, Liu X, Wang R, et al. Monocyte-derived leukemia-associated macrophages facilitate extramedullary distribution of T-cell acute lymphoblastic leukemia cells. *Cancer Res*. 2020;80:3677–91.
37. Lecoultre M, Dutoit V, Walker PR. Phagocytic function of tumor-associated macrophages as a key determinant of tumor progression control: a review. *J Immunother Cancer*. 2020;8:e001408.
38. Shapouri-Moghaddam A, Mohammadian S, Vazini H, Taghadosi M, Esmaili SA, Mardani F, et al. Macrophage plasticity, polarization, and function in health and disease. *J Cell Physiol*. 2018;233:6425–40.
39. Janowska-Wieczorek A, Belch AR, Jacobs A, Bowen D, Padua RA, Paietta E, et al. Increased circulating colony-stimulating factor-1 in patients with preleukemia, leukemia, and lymphoid malignancies. *Blood*. 1991;77:1796–803.
40. Franzè E, Stolfi C, Troncone E, Scarozza P, Monteleone G. Role of Interleukin-34 in cancer. *Cancers (Basel)*. 2020;12:252.
41. Wang L, Zheng G, Ma C, Lin Y, Zhang H, Ma Y, et al. A special linker between macrophage and hematopoietic malignant cells: membrane form of macrophage colony-stimulating factor. *Cancer Res*. 2008;68:5639–47.
42. Schoch C, Schnittger S, Klaus M, Kern W, Hiddemann W, Haferlach T. AML with 11q23/MLL abnormalities as defined by the WHO classification: incidence, partner chromosomes, FAB subtype, age distribution, and prognostic impact in an unselected series of 1897 cytogenetically analyzed AML cases. *Blood*. 2003;102:2395–402.
43. Douglass TG, Driggers L, Zhang JG, Hoa N, Delgado C, Williams CC, et al. Macrophage colony stimulating factor: not just for macrophages anymore! A gateway into complex biologies. *Int Immunopharmacol*. 2008;8:1354–76.
44. Pixley FJ, Stanley ER. CSF-1 regulation of the wandering macrophage: complexity in action. *Trends Cell Biol*. 2004;14:628–38.
45. Chu Y, Chen Y, Guo H, Li M, Wang B, Shi D, et al. SUV39H1 regulates the progression of MLL-AF9-induced acute myeloid leukemia. *Oncogene*. 2020;39:7239–52.
46. Hu Y, Wang L, Wang R, Yang F, Wang H, Liu X, et al. Effect of IL-34 on malignant biological behavior of human acute monocytic leukemia cells. *Chin. J Cancer Biother*. 2018;25:447–54.
47. Baghdadi M, Endo H, Tanaka Y, Wada H, Seino KI. Interleukin 34, from pathogenesis to clinical applications. *Cytokine*. 2017;99:139–47.
48. Kong F, Zhou K, Zhu T, Lian Q, Tao Y, Li N, et al. Interleukin-34 mediated by hepatitis B virus X protein via CCAAT/enhancer-binding protein alpha contributes to the proliferation and migration of hepatoma cells. *Cell Prolif*. 2019;52:e12703.
49. Pabon CM, Abbas HA, Konopleva M. Acute myeloid leukemia: therapeutic targeting of stem cells. *Expert Opin Ther Targets*. 2022;26:547–56.
50. Zhang Y, Xia F, Liu X, Yu Z, Xie L, Liu L, et al. JAM3 maintains leukemia-initiating cell self-renewal through LRP5/AKT/ β -catenin/CCND1 signaling. *J Clin Invest*. 2018;128:1737–51.
51. Grey W, Rio-Machin A, Casado P, Grönroos E, Ali S, Miettinen JJ, et al. CKS1 inhibition depletes leukemic stem cells and protects healthy hematopoietic stem cells in acute myeloid leukemia. *Sci Transl Med*. 2022;14:eabn3248.
52. Hayakawa Y, Ariyama H, Stancikova J, Sakitani K, Asfaha S, Renz BW, et al. Mist1 expressing gastric stem cells maintain the normal and neoplastic gastric epithelium and are supported by a perivascular stem cell niche. *Cancer Cell*. 2015;28:800–14.
53. Gottardi M, Simonetti G, Sperotto A, Nappi D, Ghelli Luserna di Rorà A, Padella A, et al. Therapeutic targeting of acute myeloid leukemia by gemtuzumab ozogamicin. *Cancers (Basel)*. 2021;13:4566.
54. Stiehl T, Baran N, Ho AD, Marciniak-Czochra A. Cell division patterns in acute myeloid leukemia stem-like cells determine clinical course: a model to predict patient survival. *Cancer Res*. 2015;75:940–9.
55. Solh M, DeFor TE, Weisdorf DJ, Kaufman DS. Extramedullary relapse of acute myelogenous leukemia after allogeneic hematopoietic stem cell transplantation: better prognosis than systemic relapse. *Biol Blood Marrow Transpl*. 2012;18:106–12.
56. Qiao Y, Jian J, Deng L, Tian H, Liu B. Leukaemia cutis as a specific skin involvement in chronic myelomonocytic leukaemia and review of the literature: Acknowledgments. *Transl Cancer Res*. 2020;9:4988–98.
57. Krooks JA, Weatherall AG. Leukemia cutis in acute myeloid leukemia signifies a poor prognosis. *Cutis*. 2018;102:266.
58. Etzerodt A, Moulin M, Doktor TK, Delfini M, Mossadegh-Keller N, Bajenoff M, et al. Tissue-resident macrophages in omentum promote metastatic spread of ovarian cancer. *J Exp Med*. 2020;217:e20191869.

AUTHOR CONTRIBUTIONS

DZ: Conceptualization, resources, data curation, software, formal analysis, validation, investigation, writing-original draft. XC: Data curation, formal analysis, validation, investigation. YL: Data curation, formal analysis. RW: Validation, resources. HW: Data curation, validation, investigation. YD: Data curation, formal analysis. QR: Resources, supervision. LW: Resources, data curation, formal analysis. GZ: Conceptualization, supervision, funding acquisition, writing-review, and editing. All authors approved all versions including the final version, and are responsible for the accuracy and integrity of all aspects of the manuscript.

FUNDING

This work was supported by grants 81970155 and 82170174 from the National Natural Science Foundation of China (NSFC), program 2021YFA1100703 from National Key Research and Development Program of China, program 2021-12M-1-041 from the CAMS Innovation Fund for Medical Sciences (CIFMS) and grant 21JCJYJC01220 from the Tianjin Natural Science Foundation. Z.GG. is a recipient of the New Century Excellent Talents in University (NCET-08-0329).

COMPETING INTERESTS

The authors declare no competing interests.

ADDITIONAL INFORMATION

Supplementary information The online version contains supplementary material available at <https://doi.org/10.1038/s41419-023-05822-z>.

Correspondence and requests for materials should be addressed to Guoguang Zheng.

Reprints and permission information is available at <http://www.nature.com/reprints>

Publisher's note Springer Nature remains neutral with regard to jurisdictional claims in published maps and institutional affiliations.



Open Access This article is licensed under a Creative Commons Attribution 4.0 International License, which permits use, sharing, adaptation, distribution and reproduction in any medium or format, as long as you give appropriate credit to the original author(s) and the source, provide a link to the Creative Commons license, and indicate if changes were made. The images or other third party material in this article are included in the article's Creative Commons license, unless indicated otherwise in a credit line to the material. If material is not included in the article's Creative Commons license and your intended use is not permitted by statutory regulation or exceeds the permitted use, you will need to obtain permission directly from the copyright holder. To view a copy of this license, visit <http://creativecommons.org/licenses/by/4.0/>.

© The Author(s) 2023